Published in final edited form as:
Cardiovasc Eng Technol. 2012 December 1; 3(4): 424–438. doi:10.1007/s13239-012-0108-4.

Echocardiographic Characterization of Postnatal Development in Mice with Reduced Arterial Elasticity

Victoria P. Le and **Jessica E. Wagenseil**
Department of Biomedical Engineering, Saint Louis University, St. Louis, MO

Abstract

Purpose—Decreased expression of elastin results in smaller, less compliant arteries and high blood pressure. In mice, these differences become more significant with postnatal development. It is known that arterial size and compliance directly affect cardiac function, but the temporal changes in cardiac function have not been investigated in elastin insufficient mice. The aim of this study is to correlate changes in arterial size and compliance with cardiac function in wildtype (WT) and elastin haploinsufficient (*Eln*$^{+/-}$) mice from birth to adulthood.

Methods—Ultrasound scans were performed at the ages of 3, 7, 14, 21, 30, 60, and 90 days on male and female WT and *Eln*$^{+/-}$ mice. 2-D ultrasound and pulse wave Doppler images were used to measure the dimensions and function of the left ventricle (LV), ascending aorta and carotid arteries.

Results—*Eln*$^{+/-}$ arteries are smaller and less compliant at most ages, with significant differences from WT as early as 3 days old. Surprisingly, there are no correlations ($R^2 < 0.2$) between arterial size and compliance with measures of LV hypertrophy or systolic function. There are weak correlations ($0.2 < R^2 < 0.5$) between arterial size and compliance with measures of LV diastolic function.

Conclusions—*Eln*$^{+/-}$ mice have similar cardiac function to WT throughout postnatal development, demonstrating the remarkable ability of the developing cardiovascular system to adapt to mechanical and hemodynamic changes. Correlations between arterial size and compliance with diastolic function show that these measures may be useful indicators of early diastolic dysfunction.

Keywords

Aorta; Carotid; Stiffness; Compliance; Diastolic dysfunction; Elastin

Introduction

Elastin is an extracellular matrix (ECM) protein important for elasticity in organs that undergo large deformations, such as the lungs and blood vessels. In the large arteries, elastin is deposited in the media by smooth muscle cells (SMCs) and cross-linked to form concentric sheets called elastic lamellae. Elastin deposition occurs from mid-gestation through postnatal development and is essentially nonexistent in adult animals [1]. In adult animals, elastic lamellae are degraded and fragmented with age, leading to increased stiffness of the arterial wall [2]. Arterial compliance is an inverse measure of arterial stiffness. Decreased compliance of the large arteries in humans is correlated with impaired left ventricular (LV) subendocardial function [3], concentric LV hypertrophy [4], impaired

Corresponding Author: Jessica E. Wagenseil, D.Sc., Department of Biomedical Engineering, Saint Louis University, 3507 Lindell Blvd., Saint Louis, MO 63103, Ph: 314-977-8646, Fax: 314-977-8288, jwagense@slu.edu.

LV diastolic function [5], and is an important predictor of cardiovascular mortality [6]. However, there has been limited investigation into the temporal relationship between decreased arterial compliance and cardiac function in animal models.

Williams Syndrome (WS) and Supravalvular Aortic Stenosis (SVAS) are two human diseases associated with elastin deficiency [7–8]. WS and SVAS are characterized by aortic stenoses and hypertension that can lead to eventual cardiac failure. Several varieties of genetically-modified mice have been developed to facilitate the study of these diseases, and the results show that as elastin amounts decrease, arterial diameter and compliance decrease and blood pressure increases [9–11]. These changes become more significant with postnatal development [12]. Elastin null mice (*Eln−/−*) die shortly after birth, with tortuous blood vessels occluded by overproliferating SMCs [13–14], in a process that may mimic aortic stenosis in SVAS and WS. Interestingly, mice with only small amounts of elastin (30 – 50%) are able to adapt to the mechanical and hemodynamic changes in the developing cardiovascular system and live a relatively normal lifespan.

In previous work on mice with reduced elastin amounts, comprehensive studies of cardiac function were not performed and the mechanical data were obtained from ex vivo arterial segments. Hence, the objective of this study is to quantify in vivo cardiovascular and cardiac parameters in wildtype (WT) and $Eln^{+/-}$ mice from birth to adulthood using echocardiography. We hypothesize that reduced arterial size and compliance in *Eln+/−* mice will affect cardiac function during postnatal growth and development. Changes may include cardiac hypertrophy (chamber dilation and wall thickening), systolic dysfunction (reduced contractility and ejection), or diastolic dysfunction (reduced relaxation and filling). Elucidation of the relationships between arterial size, compliance and cardiac function in an animal model may help inform diagnostic and treatment protocols for humans with cardiac and cardiovascular disease.

Methods

Mice

$Eln^{+/-}$ and WT littermates in the C57BL6 background [14] were bred in the institutional animal facility. Mice were used at the ages of 3, 7, 14, 21 – 24 (21), 30 – 34 (30), 60 – 64 (60) and 90 – 94 (90) days (d) for cardiac and cardiovascular ultrasound examination. Some mice were used at multiple time points, while others were sacrificed after scanning for other studies [15–17]. Both male and female mice were used in the study. All protocols were approved by the Saint Louis University Institutional Animal Care and Use Committee.

Preparation

All mice were weighed prior to the ultrasound examination. The mice were placed in an induction chamber with 2.5% isoflurane, and then transferred to a table, where they continued to receive 2.5% isoflurane via nose cone. Petroleum-based lubricant was applied to their eyes to prevent desiccation. A chemical hair remover was used to depilate the chests of mice from 14 – 90d, and warm water was used to rinse off the hair remover. The mice were then transferred to the ultrasound imaging platform, where they received 1.5% isoflurane for the duration of the 10 – 15 minute examination. The mice were secured at their extremities to the ultrasound platform with surgical tape. The hands and feet of mice from 21 – 90d were coupled to ECG contacts on the platform. Younger animals were too small for the ECG contacts. Body temperature in 14 – 90d animals was maintained at 37.5 C with a heat lamp combined with the heated platform of the Integrated Rail System (VisualSonics, Toronto, Canada) and monitored using a digital rectal probe. 3 and 7d mice were examined quickly after separation from their mothers. Their temperature could not be

monitored due to rectal probe size limitations. Examinations of 3 and 7d mice were performed with a heat lamp, the heated platform set at 40 C and a gauze pad placed between the pups and platform. Following examination, 3 – 14d pups were cleaned and returned to their mothers.

Echo Machine

Examinations were performed with the Vevo 770 High Resolution Imaging System (VisualSonics, Toronto, Canada). The transducers used are outlined in Online Resource 1. Measurements were performed manually using VisualSonics software. All data points were averaged from measurements made in triplicate by a user blinded to the genotype using mouse echocardiography conventions [18].

Echocardiographic Examination

Examinations were performed on mice secured in the supine position. Pre-warmed coupling gel (Parker Aquasonic 100) was used. The imaging views, abbreviations, sources of dimensional measurements and calculations are outlined in Table 1, which is based on a previously-published protocol [19]. LV mass (LVM) was calculated using the Penn algorithm: $LVM = 1.05*[(IVST + LVIDd + PWT)^3 - (LVIDd)^3]$, where IVST is the interventricular septum thickness, LVIDd is the LV inner diameter at end-diastole, and PWT is the posterior wall thickness [20]. Because of the irregular shape of the $Eln^{+/-}$ ascending aorta, it was difficult to obtain views of the aorta in $Eln^{+/-}$ animals from the traditional aortic arch view. When the aorta could not be visualized from the traditional view, an alternate image was obtained by tilting the platform such that the animal's head was pointed down and approaching the animal's ascending aorta with the scanhead held vertically, the notch pointed at the animal's head. This view is termed the modified parasternal long axis (MPSLAX) in Table 1 and was used for both WT and $Eln^{+/-}$ mice whenever a satisfactory M-mode image of the aortic arch could not be obtained. Preliminary comparisons did not show any significant differences between the measurements taken from this view or the traditional aortic arch view. Mitral valve inflow measurements were taken using an angle of interrogation that ranged from 8 to 14 degrees. Velocity Time Integral (VTI) and mean velocity of the aortic valve were measured from pulse wave Doppler readings taken at the aortic root. Aortic valve diameter measurements were taken at the supra-aortic ridge. Cardiac output (CO) was calculated from the following formula: CO = LV outflow tract VTI $\times$ $(\text{diameter}/2)^2 \times 3.14 \times$ heart rate, to avoid making assumptions about the LV geometry [21].

Statistics

Data are presented as mean ± standard deviation. Because it was not possible to examine all mice at every age, each mouse at each time point was treated as a separate data point and repeated measures or paired comparisons were not taken into account in the statistical analysis. A general linear model (GLM) was used to determine the effects of age, sex, and genotype, and all interactions between these factors on the measured parameters. WT and $Eln+/-$ mice were divided into groups by age, as age always had a significant effect in the GLM, and by sex only if sex had a significant effect in the GLM. Because genotype differences are the primary focus of the study, two-tailed t-tests assuming unequal variance were used to further investigate significant differences between WT and $Eln^{+/-}$ mice when genotype had a significant effect in the GLM. Additionally, linear regression analyses were performed to determine correlations between independent measures of arterial size or compliance and measures of cardiac function. All analyses were performed with SPSS software (IBM). $P < 0.05$ was considered significant, $R^2 > 0.7$ was considered a strong correlation, $0.7 > R^2 > 0.5$ was considered a correlation, $0.5 > R^2 > 0.2$ was considered a weak correlation, and $R^2 < 0.2$ was considered no correlation.

Results

All results for the significant effects of age, sex, genotype, and the interactions between factors are shown in Table 2 and discussed briefly below. The number of mice used for each measurement is given in Online Resource 2. The groups were divided by sex only if sex had a significant effect in the GLM. Additional results for significant differences between genotypes are discussed below and shown in the referenced figures. All figures show results for each genotype at every age, but only show separate results for male and female mice if sex had a significant effect in the GLM.

Body weight (BW) and left ventricular mass (LVM)

BW is significantly affected by age and sex, while LVM is significantly affected by age, sex, and genotype (Table 2). From 3 to 90d, BW increases about 12-fold (Fig. 1A), while LVM increases about 25-fold (Fig. 1B). Normalized LV mass (LVM/BW) is significantly affected by age and genotype, but not by sex (Table 2). LVM/BW increases in early postnatal development (3 – 14d) and declines in early adulthood (21 – 90d), so that 3 and 90d values are approximately equal (Fig. 1C). Although the GLM shows a significant effect of genotype on both LVM and LVM/BW, there are no significant differences between genotypes at any age when compared using a t-test.

Left ventricular dimensions

Left ventricular inner diameter (LVID) at diastole and systole and fractional shortening (FS) are significantly affected by age, but not by sex or genotype (Table 2). LVID increases about 2.5-fold (Fig. 2A) and FS remains approximately constant around 30% from 3 to 90d (Fig. 2B). Fig 2C shows a representative LV short axis m-mode image for a 14d WT mouse.

Arterial dimensions and compliance

The ascending aorta inner diameter (ASID) at diastole and systole are significantly affected by age and genotype, but not by sex (Table 2). ASID is 7 – 15% smaller in $Eln^{+/-}$ mice than WT starting at age 7d ($p < .001 – .018$) (Fig 3A). The percent increase in diameter from diastole to systole (ASID % increase), which is a non-traditional measure of aortic compliance, is significantly affected by age and genotype, but not by sex (Table 2). ASID % increase is reduced 17 – 46% in $Eln^{+/-}$ mice at age 3d and above, except for ages 14 and 21d ($p < .001 – .034$) (Fig 3B). Aortic compliance is traditionally defined as the change in diameter divided by the change in pressure. Blood pressure was not measured in this study, but was measured previously at similar ages for WT and $Eln^{+/-}$ mice [16]. The previous results show that $Eln^{+/-}$ mice have increased pulse pressure at age 21d and above, which would increase the compliance differences between genotypes in Fig. 3B. Example m-mode images of 3d aortas are shown in Fig 3C–D. The branches of the $Eln^{+/-}$ aortic arch extend at angles that are noticeably different from those of WT animals (Fig. 3E–F for 14d animals, see also the video in Online Resource 3). The angle differences were not quantified due to the difficulty in obtaining clear images of the branches in all mice.

Carotid artery inner diameter (CAID) at diastole and systole are significantly affected by age and genotype, but not by sex (Table 2). CAID is 8 – 16% smaller in $Eln^{+/-}$ mice than WT at age 7d and above ($p < .001 – .03$) (Fig 4A). The percent increase in diameter from diastole to systole (CAID % increase), which is a non-traditional measure of arterial compliance, is significantly affected by age and genotype, but not by sex (Table 2). CAID % increase is reduced 13 – 33% in $Eln^{+/-}$ mice at age 14d and above, except for age 60d ($p < .001 – .023$) (Fig 4B). As with the aortic compliance, including the published pressure differences [16] in the carotid compliance calculations would increase the compliance differences between genotypes. Example m-mode images of 3d carotids are shown in Fig 4C–D.

Cardiac output

Aortic valve diameter at systole (AVDs) is significantly affected by age, sex, and genotype (Table 2). AVDs is about 10% smaller in male and female *Eln*$^{+/-}$ mice compared to WT at 30 and 60d ($p = .004 – .049$). Female *Eln+/−* mice at 90d have 14% smaller AVDs than WT ($p < .001$) (Fig 5A). Heart rate is significantly affected by age and sex, but not by genotype (Table 2). Heart rate increases about 1.5-fold between 3 and 90d (Fig 5B). Cardiac output (CO) is significantly affected by age, sex, and genotype (Table 2). CO is 18 – 27% lower in *Eln*$^{+/-}$ compared to WT mice for females at 60d and 90d and males at 60d ($p = .009 – .035$) (Fig. 5C). An example aortic valve VTI tracing for a 3d mouse is shown in Fig. 5D and example aortic valves diameters taken at the supra-aortic ridge for 30d mice are shown in Fig. 5E – F.

Stroke volume (SV) and ejection fraction (EF)

LV volume at diastole (LVVd) is significantly affected by age and sex, but not by genotype (Table 2). LVVd increases about 15-fold in male mice and 10-fold in female mice between 3 and 90d (Fig. 6A). LVV at systole (LVVs) is significantly affected by age, sex, and genotype (Table 2). LVVs is 28% lower in male *Eln*$^{+/-}$ mice compared to WT at 7d ($p = .003$) and 26–29% lower in female *Eln+/−* mice compared to WT at 14 and 21d ($p = .019$ and .001, respectively) (Fig. 6B). SV is significantly affected by age and sex, but not by genotype (Table 3). SV increases about 12-fold in male mice and 8-fold in female mice between 3 and 90d (Fig 6C). EF is significantly affected by age and genotype, but not by sex (Table 2). EF is increased 17% in *Eln*$^{+/-}$ mice compared to WT at 14d ($p = .001$) (Fig. 6D). Example LV tracings for a 3d WT mouse are shown in Fig. 6E – F.

Diastolic filling

The peak mitral valve velocities of early rapid filling (MV E) and atrial filling (MV A) are significantly affected by age, but not by sex or genotype (Table 2). Both velocities increase about 2-fold between 3 and 30d and then remain approximately constant (Fig. 7A–B). The E/A ratio is significantly affected by age and genotype, but not by sex (Table 2). The E/A ratio is 10–14% lower in *Eln*$^{+/-}$ mice compared to WT at 14 and 21d ($p = .015$ and .035, respectively) (Fig. 7C). Isovolumic relaxation time (IVRT) is significantly affected by age, but not by sex or genotype (Table 2). IVRT decreases about 35% between 3 and 14d before remaining approximately constant (Fig 7D). Example measurements for MV E, MV A and IVRT in a 3d WT mouse are shown in Fig 7E.

Regression analyses

Linear regression analyses were used to investigate correlations between measures of arterial size and compliance and measures of cardiac function for all of the data combined. The possible measures of arterial size and compliance include: ASIDdias, ASIDsyst, ASID % increase, CAIDdias, CAIDsyst, CAID % increase and AVDs. There are significant correlations between most of these variables, therefore AVDs and CAID % increase were investigated as independent, uncorrelated ($R^2 = .000$) measures of arterial size and compliance, respectively. For cardiac function, LVM/BW was chosen as a measure of cardiac hypertrophy, FS and EF were chosen as measures of systolic function and E/A ratio and IVRT were chosen as measures of diastolic function. AVDs and CAID % increase have no correlation ($R^2 < 0.2$) with LVM/BW, FS or EF. AVDs has no correlation with E/A ratio, although CAID % increase has a weak correlation ($R^2 = .265$) (Fig. 8A). CAID % increase has no correlation with IVRT, but AVDs has a weak correlation ($R^2 = .243$) (Fig. 8B).

Discussion

Elastin and cardiac/cardiovascular growth

The size and performance of the cardiac and cardiovascular system in WT and *Eln*$^{+/-}$ mice was examined throughout postnatal development using ultrasound. During this period, the mouse and its organs, including the heart and arteries, grow in size. Measures of size, including BW, LVM, LVID, ASID, CAID, AVD, and LVV, increase with age. By 30d, both genotypes have reached a growth plateau with minimal changes in LV size or arterial dimensions, although there are still some changes in BW. In comparing genotypes, there are no significant differences in BW or measures of cardiac size, but as early as 7d there are significant differences in arterial dimensions. From 3 – 30d, *Eln*$^{+/-}$ arteries grow at a slower rate to produce smaller arteries for every age at 7d and above. The measurements in WT mice are consistent with previous in vivo and ex vivo measurements on young mice [22, 12, 23–24, 19–20]. The growth trends are qualitatively similar to humans [25–26].

The arterial wall is composed of ECM proteins and SMCs. In the *Eln*$^{+/-}$ mouse, the SMCs can only produce half as much elastin [27], but still need to produce an ECM with the necessary mechanical properties for normal cardiovascular function. One strategy to accommodate less elastin is to decrease the total wall volume to maintain the ratio of elastin to other proteins in the wall. The wall volume cannot be decreased so much that the wall thickness is too small to withstand the internal pressures or the inner diameter is too small to allow normal cardiac output and distribute blood to distal tissues. The smaller size of *Eln*$^{+/-}$ arteries may represent the optimal balance between maintaining wall properties and blood distribution.

Elastin and cardiac/cardiovascular function

Measures of cardiac hypertrophy, systolic and diastolic function were determined for WT and *Eln*$^{+/-}$ mice at different postnatal ages. Cardiac hypertrophy was determined by LVM/BW measurements using the Penn algorithm [20], which includes measures of both the LV chamber and wall dimensions. Systolic function was investigated through EF and FS calculations, which measure how efficiently the LV contracts to eject blood. Diastolic function was examined through E/A ratio and IVRT, which are related to how efficiently the LV relaxes to fill with blood. While systolic dysfunction is generally defined as a decrease in EF, diastolic dysfunction is more complicated to define. Early stage (grade 1) diastolic dysfunction is characterized by reduced E/A ratio, however late stage (grade 3) is characterized by an increased E/A ratio, hence moderate stage (grade 2) is characterized by a pseudonormal E/A ratio [28]. IVRT will increase with diastolic dysfunction, but is significantly affected by preload which may be independent of changes in LV relaxation [29]. The functional measurements in WT mice are consistent with previous ultrasound studies on young mice [19, 24, 22, 20]. Most of the measures, including LVM/BW, FS, HR, SV, and IVRT are significantly affected by age, but not by genotype. Despite significant changes in arterial size and compliance, there are limited effects on cardiac function in young *Eln*$^{+/-}$ mice. These results demonstrate the remarkable ability of the developing cardiovascular system to adapt to changes in hemodynamics and mechanics.

Three of the measures, CO, EF, and E/A ratio, are significantly affected by age and genotype. CO was calculated from the aortic valve VTI and dimensions and is directly affected by the smaller arterial size in *Eln*$^{+/-}$ mice. EF was calculated from LV volume measurements, which assume an ellipsoidal geometry. CO can also be calculated by SV x HR, which depends directly on the LV volume measurements. When CO is calculated this way, similar trends with age as Fig. 5C are obtained, but there are no longer significant differences between WT and *Eln*$^{+/-}$ mice at the older ages. Hence, uncertainties in

ultrasound data measurements and assumptions can skew the statistical conclusions, but it is clear that CO is maintained near WT levels in $Eln^{+/-}$ mice throughout most of postnatal development. EF is significantly greater in $Eln^{+/-}$ mice at 14d, indicating that systolic cardiac function is not compromised by the arterial changes, and may even be enhanced. E/A ratio is significantly lower in $Eln^{+/-}$ mice compared to WT at 14 and 21d and is caused by slight, opposite changes in the magnitude of the E and A wave velocity, because MV E and MV A individually are not affected by genotype. A decrease in E/A ratio indicates early diastolic dysfunction [29]. The LV myocardium itself contains elastin and alterations in elastin amount or elastin to collagen ratio may independently affect diastolic function [30]. It is difficult to study the effects of elastin deficiency on the heart without considering secondary effects from the arteries. Cardiac specific reduction of elastin in genetically-modified mice may help determine the direct role of elastin in cardiac function [31].

Arterial function was examined by determining the percent change from diastole to systole of the inner diameters of the ascending aorta and carotid artery. This is a non-traditional measure of arterial compliance and an inverse measure of arterial stiffness. The percent increase in both arteries is significantly affected by age and genotype. The compliance increases after birth, peaking around 21d in the aorta and 14 – 21d in the carotid for both genotypes. The arterial compliance differences with postnatal age follow a very similar pattern to elastin gene expression. In the WT mouse thoracic aorta, elastin expression begins approximately nine days before birth, increases dramatically after birth until about 14d, then decreases to baseline levels throughout adulthood [1]. Protein quantification data confirm that elastin amounts peak around 21 – 30d in WT and *Eln+/−* aorta [32], soon after elastin expression begins to decline. It is possible that elastin deposition drives the large increase in compliance during the early postnatal period. The compliance then returns to baseline levels around 21d as the wall continues to thicken and grow without additional elastin deposition. Differences in elastin amounts between WT and *Eln+/−* aorta are not significant until 21d [32], while differences in compliance are significant between genotypes as early as 3d in the aorta and 14d in the carotid. Functional differences may be measurable earlier than protein amounts due to the difficulty in measuring small elastin amounts in newborn mouse aorta. The timing of the significant reductions in compliance for each artery are consistent with previous ex vivo data [12]. The timing suggests that lower levels of elastin affect the mechanics first in arteries with the highest elastin content, since elastin amounts decrease with distance from the heart [33].

Correlations between arterial size or compliance and cardiac function

Reduced arterial compliance, or increased arterial stiffness, is correlated with LV hypertrophy and decreased systolic and/or diastolic function in humans [4, 3, 5]. Reduced arterial size is also correlated with changes in LV function in humans, particularly in extreme cases such as aortic stenoses [34–36]. The changes in arterial compliance and size with postnatal development and genotype in this study offer a unique opportunity to examine correlations between these parameters and different measures of cardiac function in an animal model. It was expected that as arterial size or compliance decreased, LVM/BW would increase indicating LV hypertrophy, EF and FS would decrease indicating systolic dysfunction, while E/A ratio would decrease and IVRT would increase indicating early diastolic dysfunction. Surprisingly, LVM/BW, EF and FS have no correlation with either arterial size or compliance. These results imply that reduced arterial size and compliance have no negative effects on LV hypertrophy and systolic function in WT and $Eln^{+/-}$ mice. Importantly, when viewed in light of normal development, they may even have positive effects, stimulating remodeling to adapt to arterial changes and maintain cardiac function.

Although the finding that decreased arterial compliance does not correlate with LV hypertrophy is unexpected, there is evidence that LV wall thickness does not correlate with

arterial compliance in young humans, but only in older individuals [37]. This implies that young individuals may be better able to adapt to cardiovascular changes than older individuals. Decreased arterial compliance is often related to LV hypertrophy through its relationship with high blood pressure. In growing children and young adults, LV mass is most strongly correlated with body weight, and only weakly affected by systolic blood pressure [25, 38–39]. It has been argued that growth due to increases in body weight represent a greater physiologic stress on the heart than increases in blood pressure in a young, healthy population. Determining the time period and limits of this hypothesized adaptation process will be important in making treatment decisions for younger individuals with cardiovascular disease.

Our finding that decreased arterial compliance does not correlate with changes in systolic function is less surprising. There are examples of individuals with decreased arterial compliance and high blood pressure, but with normal systolic function (as defined by preserved EF). These individuals often have evidence of diastolic dysfunction at various stages [40–42]. The combination of decreased E/A ratio and increased IVRT in this study suggest that decreased arterial size and compliance correlate with early diastolic dysfunction [29, 43]. In a study of human subjects without known cardiovascular disease, E/A ratio was also significantly correlated with carotid artery compliance [5]. The authors suggest a continuum relationship between arterial compliance and LV diastolic function and this study shows that both normal and genetically-modified mice operate on a similar continuum during postnatal development and may be useful models for further investigating the relationships between arterial size and compliance and diastolic dysfunction.

Differences between humans and mice

While *Eln*$^{+/-}$ mice allow detailed temporal studies that are difficult to perform in humans, important differences must be pointed out. The small size, rapid heart rate, and orientation of the mouse heart make echocardiography challenging. Systolic function measurements have been correlated with physiologic changes in the heart, but the physiologic relevance of many diastolic function measurements in the mouse remains unclear [44]. Humans and mice with elastin haploinsufficiency develop hypertension and smaller, less compliant arteries with an increased number of elastic lamellae. The number of lamellae increases about 2.5 times in the human aorta and about 1.3 times in the mouse aorta [27], and may be a remodeling response to maintain the tension/lamellar unit [45]. The difference in the number of added units and the fact that *Eln*$^{+/-}$ mice do not develop aortic stenoses, suggest a fundamental difference in the extent of the remodeling response and this may affect remodeling of the cardiac and cardiovascular system in general. Other mouse models with alterations in arterial size and/or compliance, such as mice lacking fibulin 5, which have decreased arterial compliance, but no changes in the number of lamellar units [46–47], can be used to provide further support for the current studies. Of course, all results in animals must eventually be confirmed in clinical studies.

Limitations

This study was limited to ages from birth to adulthood in mice. Aged mice [48] may provide additional data for comparison to complications in human aging. Seven different age groups were examined in this study, and it was not possible to collect optimal images for every mouse. The images for some age groups were more difficult to obtain than others, for example clear AVDs images were difficult to get in 3 and 7d old pups. Power analyses were conducted to estimate the minimum required mouse numbers for each measurement without taking sex into account. For some measurements, males and females were separated based on the results of the GLM, decreasing the number of animals per group, and reducing statistical power, but this is usually only for one group per measurement. Ultrasound probes

of differing focal depths and resolutions were used for each age group. However, the probes have approximately the same percent resolution based on the changing size of the LV with age and the probes were consistent at specific ages between genotypes. The percent change in diameter was used as a non-traditional measure of arterial compliance and an inverse measure of arterial stiffness instead of more traditional methods, such as pulse wave velocity (PWV) or compliance calculations that involve pressure measurements. Blood pressures have previously been measured in WT and $Eln^{+/-}$ mice at similar ages [12] and the results indicate that including pressure differences would magnify the compliance differences in the current study. The study results highlight early diastolic function differences, but diastolic dysfunction is a complicated disease with changes in numerous cardiac parameters [49]. Future work must include additional measures of diastolic function, such as pulse wave Doppler tissue imaging (TDI) [50].

Conclusions

Reduced elastin amounts lead to significantly reduced arterial size and compliance in $Eln^{+/-}$ mice compared to WT as early as 3d of age. Despite these cardiovascular differences, measures of LV hypertrophy and most measures of LV systolic function are not significantly different between WT and $Eln^{+/-}$ mice, highlighting the capacity of the developing cardiovascular system to adapt to mechanical and hemodynamic changes. In contrast, LV diastolic function, as measured by E/A ratio, is significantly affected by genotype and the differences are highest during the same period that carotid artery compliance differences are the highest, suggesting that the developing cardiovascular system may not be able to adapt LV diastolic function as well as systolic function when challenged. There is a weak correlation between arterial compliance and E/A ratio and between arterial size and IVRT, another measure of diastolic function. The correlations suggest that reduced arterial size and compliance may be an early predictor of impaired LV diastolic function in mice.

Supplementary Material

Refer to Web version on PubMed Central for supplementary material.

Acknowledgments

This work was funded, in part, by National Institutes of Health grants R00 HL087653, R01 HL105314, and R01 HL115560. Dr. Robert Mecham at the Washington University School of Medicine is gratefully acknowledged for providing the $Eln^{+/-}$ mice. The Saint Louis University Center for Cardiovascular Research is gratefully acknowledged for providing the ultrasound equipment.

References

1. Kelleher CM, McLean SE, Mecham RP. Vascular extracellular matrix and aortic development. Curr Top Dev Biol. 2004; 62:153–88. [PubMed: 15522742]
2. Greenwald SE, Moore JE Jr, Rachev A, Kane TP, Meister JJ. Experimental investigation of the distribution of residual strains in the artery wall. J Biomech Eng. 1997; 119(4):438–44. [PubMed: 9407283]
3. Vinereanu D, Nicolaides E, Boden L, Payne N, Jones CJ, Fraser AG. Conduit arterial stiffness is associated with impaired left ventricular subendocardial function. Heart. 2003; 89(4):449–50. [PubMed: 12639882]
4. Palmieri V, Bella JN, Roman MJ, Gerdts E, Papademetriou V, Wachtell K, et al. Pulse pressure/stroke index and left ventricular geometry and function: the LIFE Study. J Hypertens. 2003; 21(4): 781–7.10.1097/01.hjh.0000052491.18130.dc [PubMed: 12658025]
5. Vriz O, Bossone E, Bettio M, Pavan D, Carerj S, Antonini-Canterin F. Carotid artery stiffness and diastolic function in subjects without known cardiovascular disease. Journal of the American

Society of Echocardiography : official publication of the American Society of Echocardiography. 2011; 24(8):915–21.10.1016/j.echo.2011.05.001 [PubMed: 21704497]

6. McEniery CM, Wilkinson IB, Avolio AP. Age, hypertension and arterial function. Clinical and experimental pharmacology & physiology. 2007; 34(7):665–71.10.1111/j.1440-1681.2007.04657.x [PubMed: 17581227]
7. Ewart AK, Morris CA, Ensing GJ, Loker J, Moore C, Leppert M, et al. A human vascular disorder, supravalvular aortic stenosis, maps to chromosome 7. Proc Natl Acad Sci U S A. 1993; 90(8):3226–30. [PubMed: 8475063]
8. Osborne LR, Martindale D, Scherer SW, Shi XM, Huizenga J, Heng HH, et al. Identification of genes from a 500-kb region at 7q11.23 that is commonly deleted in Williams syndrome patients. Genomics. 1996; 36(2):328–36.10.1006/geno.1996.0469 [PubMed: 8812460]
9. Faury G, Pezet M, Knutsen R, Boyle W, Heximer S, McLean S, et al. Developmental adaptation of the mouse cardiovascular system to elastin haploinsufficiency. J Clin Invest. 2003; 112(9):1419–28.10.1172/JCI19028 [PubMed: 14597767]
10. Hirano E, Knutsen RH, Sugitani H, Ciliberto CH, Mecham RP. Functional rescue of elastin insufficiency in mice by the human elastin gene: implications for mouse models of human disease. Circ Res. 2007; 101(5):523–31. [PubMed: 17626896]
11. Wagenseil JE, Nerurkar NL, Knutsen RH, Okamoto RJ, Li DY, Mecham RP. Effects of elastin haploinsufficiency on the mechanical behavior of mouse arteries. Am J Physiol Heart Circ Physiol. 2005; 289(3):H1209–17.10.1152/ajpheart.00046.2005 [PubMed: 15863465]
12. Le V, Knutsen R, Mecham R, Wagenseil J. Decreased aortic diameter and compliance precedes blood pressure increases in postnatal development of elastin-insufficient mice. Am J Physiol Heart Circ Physiol. 2011; 301(1):H221–9.10.1152/ajpheart.00119.2011 [PubMed: 21536846]
13. Wagenseil JE, Ciliberto CH, Knutsen RH, Levy MA, Kovacs A, Mecham RP. Reduced vessel elasticity alters cardiovascular structure and function in newborn mice. Circ Res. 2009; 104(10): 1217–24.10.1161/CIRCRESAHA.108.192054 [PubMed: 19372465]
14. Li DY, Brooke B, Davis EC, Mecham RP, Sorensen LK, Boak BB, et al. Elastin is an essential determinant of arterial morphogenesis. Nature. 1998; 393(6682):276–80. [PubMed: 9607766]
15. Cheng JK, Mecham RP, Wagenseil JE. A fiber-based constitutive model predicts changes in amount and organization of matrix proteins with development and disease in the mouse aorta. Biomech Model Mechanobiol. 2012 Accepted.
16. Le VP, Knutsen RH, Mecham RP, Wagenseil JE. Decreased aortic diameter and compliance precedes blood pressure increases in postnatal development of elastin-insufficient mice. Am J Physiol Heart Circ Physiol. 2011; 301(1):H221–9.10.1152/ajpheart.00119.2011 [PubMed: 21536846]
17. Webster, A.; Le, VP.; Wagenseil, JE., editors. Biomedical Engineering Society Annual Meeting. Austin, TX: 2010. Quantifying elastin, collagen and total protein in mouse arteries.
18. Pollick C, Hale SL, Kloner RA. Echocardiographic and cardiac Doppler assessment of mice. Journal of the American Society of Echocardiography : official publication of the American Society of Echocardiography. 1995; 8(5 Pt 1):602–10. [PubMed: 9417202]
19. Bose AK, Mathewson JW, Anderson BE, Andrews AM, Martin Gerdes A, Benjamin Perryman M, et al. Initial experience with high frequency ultrasound for the newborn C57BL mouse. Echocardiography. 2007; 24(4):412–9. [PubMed: 17381652]
20. Ghanem A, Roll W, Hashemi T, Dewald O, Djoufack PC, Fink KB, et al. Echocardiographic assessment of left ventricular mass in neonatal and adult mice: accuracy of different echocardiographic methods. Echocardiography. 2006; 23(10):900–7.10.1111/j.1540-8175.2006.00323.x [PubMed: 17069614]
21. Finsen AV, Christensen G, Sjaastad I. Echocardiographic parameters discriminating myocardial infarction with pulmonary congestion from myocardial infarction without congestion in the mouse. J Appl Physiol. 2005; 98(2):680–9.10.1152/japplphysiol.00924.2004 [PubMed: 15475595]
22. Baumann PQ, Sobel BE, Tarikuz Zaman AK, Schneider DJ. Gender-dependent differences in echocardiographic characteristics of murine hearts. Echocardiography. 2008; 25(7):739–48.10.1111/j.1540-8175.2008.00680.x [PubMed: 18422663]

23. Huang Y, Guo X, Kassab GS. Axial nonuniformity of geometric and mechanical properties of mouse aorta is increased during postnatal growth. Am J Physiol Heart Circ Physiol. 2006; 290(2):H657–64. [PubMed: 16172154]
24. Hinton RB Jr, Alfieri CM, Witt SA, Glascock BJ, Khoury PR, Benson DW, et al. Mouse heart valve structure and function: echocardiographic and morphometric analyses from the fetus through the aged adult. Am J Physiol Heart Circ Physiol. 2008; 294(6):H2480–8.10.1152/ajpheart.91431.2007 [PubMed: 18390820]
25. Urbina EM, Gidding SS, Bao W, Pickoff AS, Berdusis K, Berenson GS. Effect of body size, ponderosity, and blood pressure on left ventricular growth in children and young adults in the Bogalusa Heart Study. Circulation. 1995; 91(9):2400–6. [PubMed: 7729027]
26. Pettersen MD, Du W, Skeens ME, Humes RA. Regression equations for calculation of z scores of cardiac structures in a large cohort of healthy infants, children, and adolescents: an echocardiographic study. Journal of the American Society of Echocardiography : official publication of the American Society of Echocardiography. 2008; 21(8):922–34.10.1016/j.echo.2008.02.006 [PubMed: 18406572]
27. Li DY, Faury G, Taylor DG, Davis EC, Boyle WA, Mecham RP, et al. Novel arterial pathology in mice and humans hemizygous for elastin. J Clin Invest. 1998; 102(10):1783–7. [PubMed: 9819363]
28. Hamlin SK, Villars PS, Kanusky JT, Shaw AD. Role of diastole in left ventricular function, II: diagnosis and treatment. American journal of critical care : an official publication, American Association of Critical-Care Nurses. 2004; 13(6):453–66. quiz 67–8.
29. Nagueh SF. Echocardiographic assessment of left ventricular relaxation and cardiac filling pressures. Current heart failure reports. 2009; 6(3):154–9. [PubMed: 19723456]
30. Mujumdar VS, Tyagi SC. Temporal regulation of extracellular matrix components in transition from compensatory hypertrophy to decompensatory heart failure. J Hypertens. 1999; 17(2):261–70. [PubMed: 10067796]
31. Fomovsky GM, Thomopoulos S, Holmes JW. Contribution of extracellular matrix to the mechanical properties of the heart. Journal of molecular and cellular cardiology. 2010; 48(3):490–6.10.1016/j.yjmcc.2009.08.003 [PubMed: 19686759]
32. Cheng JK, Stoilov I, Mecham RP, Wagenseil JE. A fiber-based constitutive model predicts changes in amount and organization of matrix proteins with development and disease in the mouse aorta. Biomech Model Mechanobiol. 201210.1007/s10237-012-0420-9
33. Greenwald SE. Ageing of the conduit arteries. The Journal of pathology. 2007; 211(2):157–72.10.1002/path.2101 [PubMed: 17200940]
34. Adda J, Mielot C, Giorgi R, Cransac F, Zirphile X, Donal E, et al. Low-Flow, Low-Gradient Severe Aortic Stenosis Despite Normal Ejection Fraction Is Associated with Severe Left Ventricular Dysfunction as Assessed by Speckle-Tracking Echocardiography: A Multicenter Study. Circulation Cardiovascular imaging. 201110.1161/CIRCIMAGING.111.967554
35. Carasso S, Cohen O, Mutlak D, Adler Z, Lessick J, Aronson D, et al. Relation of myocardial mechanics in severe aortic stenosis to left ventricular ejection fraction and response to aortic valve replacement. Am J Cardiol. 2011; 107(7):1052–7.10.1016/j.amjcard.2010.11.032 [PubMed: 21296330]
36. Chambers J. The left ventricle in aortic stenosis: evidence for the use of ACE inhibitors. Heart. 2006; 92(3):420–3.10.1136/hrt.2005.074112 [PubMed: 16501211]
37. Schillaci G, Mannarino MR, Pucci G, Pirro M, Helou J, Savarese G, et al. Age-specific relationship of aortic pulse wave velocity with left ventricular geometry and function in hypertension. Hypertension. 2007; 49(2):317–21.10.1161/01.HYP.0000255790.98391.9b [PubMed: 17200433]
38. Johnson GL, Kotchen JM, McKean HE, Cottrill CM, Kotchen TA. Blood pressure related echocardiographic changes in adolescents and young adults. American heart journal. 1983; 105(1): 113–8. [PubMed: 6217735]
39. Mahoney LT, Schieken RM, Clarke WR, Lauer RM. Left ventricular mass and exercise responses predict future blood pressure. The Muscatine Study. Hypertension. 1988; 12(2):206–13. [PubMed: 3410529]

40. Hwang JW, Kang SJ, Lim HS, Choi BJ, Choi SY, Hwang GS, et al. Impact of arterial stiffness on regional myocardial function assessed by speckle tracking echocardiography in patients with hypertension. Journal of cardiovascular ultrasound. 2012; 20(2):90–6.10.4250/jcu.2012.20.2.90 [PubMed: 22787526]
41. Jaroch J, Loboz Grudzien K, Bociaga Z, Kowalska A, Kruszynska E, Wilczynska M, et al. The relationship of carotid arterial stiffness to left ventricular diastolic dysfunction in untreated hypertension. Kardiologia polska. 2012; 70(3):223–31. [PubMed: 22430399]
42. Agoston-Coldea L, Mocan T, Bobar C. Arterial stiffness and left ventricular diastolic function in the patients with hypertension. Romanian journal of internal medicine = Revue roumaine de medecine interne. 2008; 46(4):313–21. [PubMed: 19480297]
43. Shapiro LM, Gibson DG. Patterns of diastolic dysfunction in left ventricular hypertrophy. British heart journal. 1988; 59(4):438–45. [PubMed: 2967087]
44. Scherrer-Crosbie M, Thibault HB. Echocardiography in translational research: of mice and men. Journal of the American Society of Echocardiography : official publication of the American Society of Echocardiography. 2008; 21(10):1083–92. S0894-7317(08)00371-4 [pii]. 10.1016/j.echo.2008.07.001 [PubMed: 18723318]
45. Faury G, Pezet M, Knutsen RH, Boyle WA, Heximer SP, McLean SE, et al. Developmental adaptation of the mouse cardiovascular system to elastin haploinsufficiency. J Clin Invest. 2003; 112(9):1419–28. [PubMed: 14597767]
46. Wan W, Yanagisawa H, Gleason RL Jr. Biomechanical and microstructural properties of common carotid arteries from fibulin-5 null mice. Ann Biomed Eng. 2010; 38(12):3605–17.10.1007/s10439-010-0114-3 [PubMed: 20614245]
47. Yanagisawa H, Davis EC, Starcher BC, Ouchi T, Yanagisawa M, Richardson JA, et al. Fibulin-5 is an elastin-binding protein essential for elastic fibre development in vivo. Nature. 2002; 415(6868):168–71. [PubMed: 11805834]
48. Pezet M, Jacob MP, Escoubet B, Gheduzzi D, Tillet E, Perret P, et al. Elastin haploinsufficiency induces alternative aging processes in the aorta. Rejuvenation Res. 2008; 11(1):97–112. [PubMed: 18173368]
49. Nagueh SF, Appleton CP, Gillebert TC, Marino PN, Oh JK, Smiseth OA, et al. Recommendations for the evaluation of left ventricular diastolic function by echocardiography. Journal of the American Society of Echocardiography : official publication of the American Society of Echocardiography. 2009; 22(2):107–33.10.1016/j.echo.2008.11.023 [PubMed: 19187853]
50. Schumacher A, Khojeini E, Larson D. ECHO parameters of diastolic dysfunction. Perfusion. 2008; 23(5):291–6.10.1177/0267659109102485 [PubMed: 19346268]

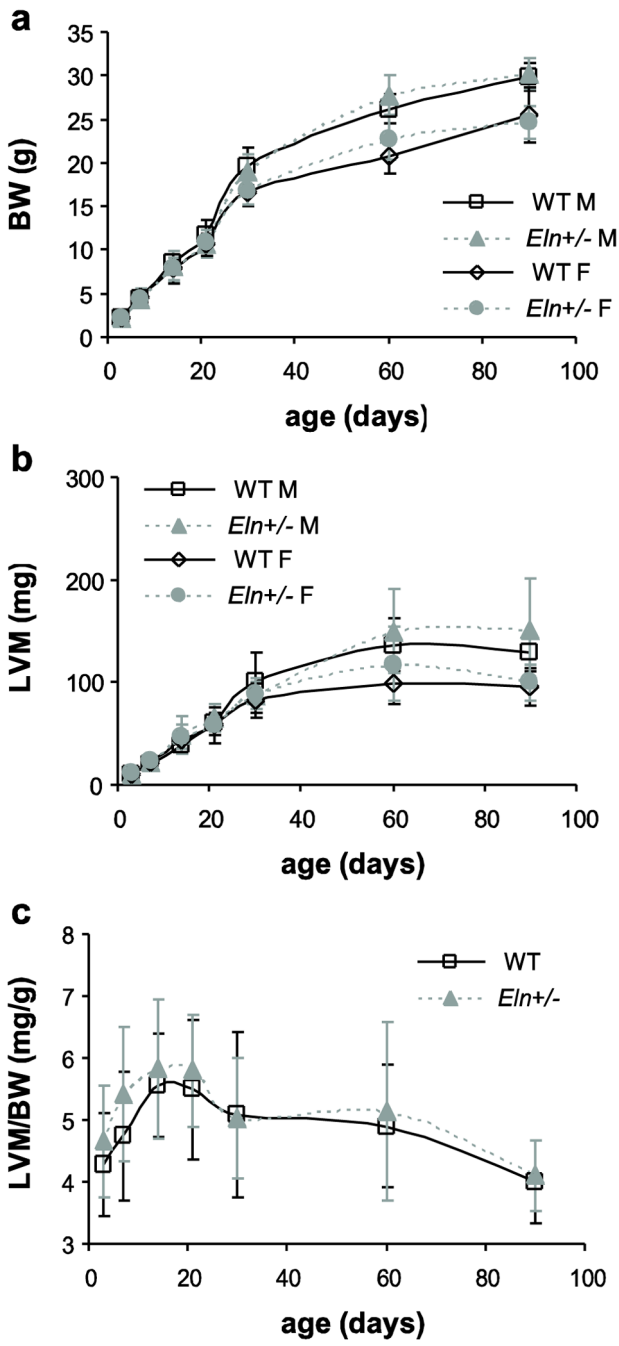

Fig. 1. Body weight (BW) and left ventricular mass (LVM)

BW (a) significantly depends on age and sex. LVM (b) significantly depends on age, sex, and genotype. The ratio of LVM/BW (c) significantly depends on age and genotype. $n = 5 – 17$ males/group, $n = 4 – 24$ females/group, $n = 10 – 26$ total/group.

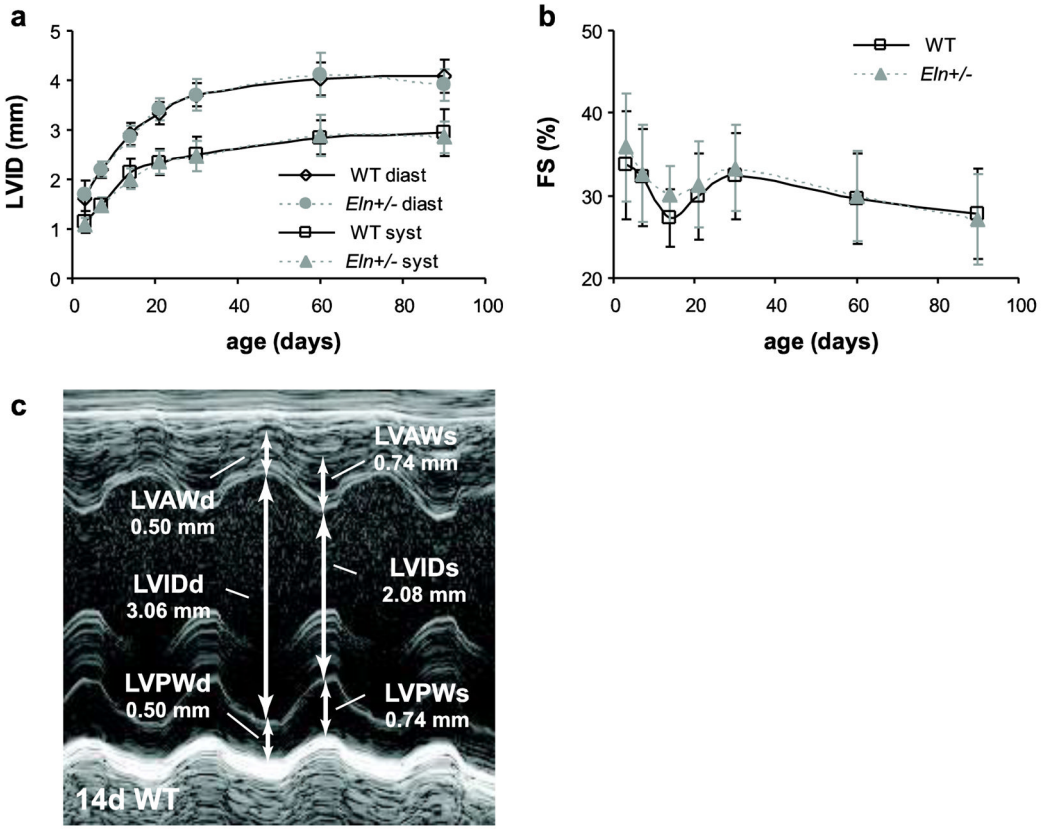

Fig. 2. Left ventricular inner diameter (LVID) and fractional shortening (FS)

LVID at diastole and systole (a) and FS (b) depend significantly on age, but not sex or genotype. Representative m-mode image and measurement in the parasternal short axis view of the LV at the mid-papillary level in a 14d WT mouse (c). d or diast = diastole; s or syst = systole. n = 10–26/group.

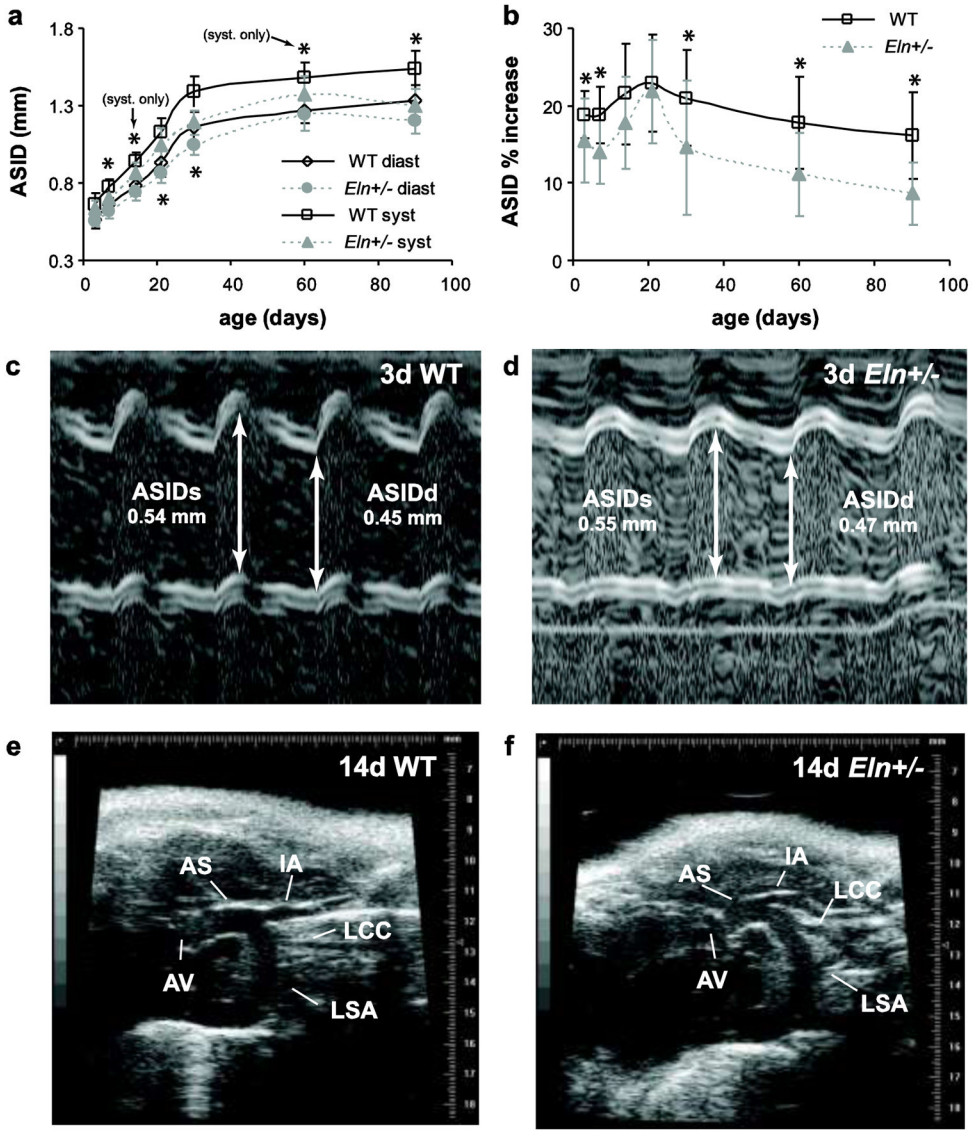

Fig. 3. Dimensions and morphology of the ascending aorta

The ascending aorta inner diameter (ASID) at diastole and systole (a) significantly depends on age and genotype, but not sex, and is 7–15% smaller in $Eln^{+/-}$ mice from age 7d and above. The percent increase from diastole to systole (b) is 17–46% less in $Eln^{+/-}$ ascending aorta from age 3d and above, except for ages 14 and 21d. Representative m-mode images and measurements of the ascending aorta in 3d WT (c) and $Eln^{+/-}$ (d) mice. Representative b-mode images of the ascending aorta at end systole for 14d WT (e) and $Eln^{+/-}$ (f) mice. d or diast = diastole; s or syst = systole; AS = ascending aorta; AV = aortic valve; IA = innominate artery; LCC = left common carotid artery; LSA = left subclavian artery. n = 13–24/group. *P < .05 between genotypes.

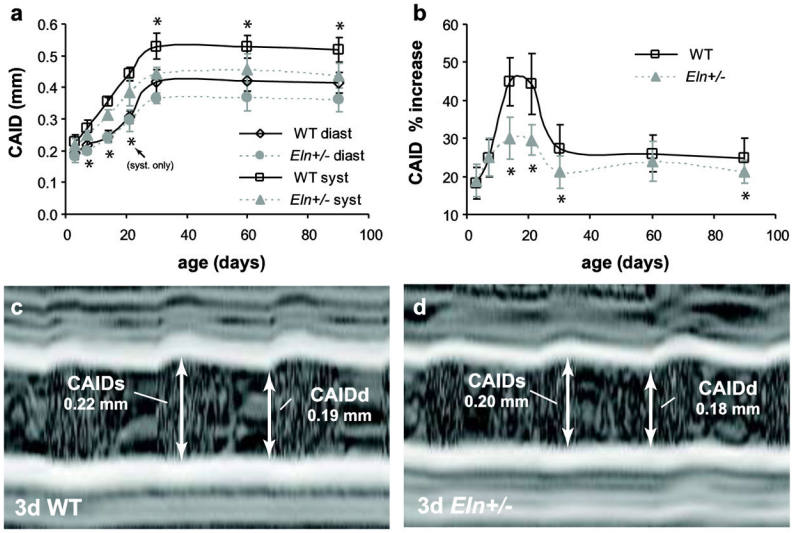

Fig. 4. Dimensions of the common carotid artery

The carotid artery inner diameter (CAID) at diastole and systole (a) significantly depends on age and genotype, but not sex, and is 8–16% smaller in *Eln+/−* mice at age 7d and above. The percent increase from diastole to systole (b) significantly depends on age and genotype, but not sex, and is 13–33% less in the carotid artery from age 14d and above, except for age 60d. Representative m-mode images and measurements of the carotid artery in 3d WT (c) and $Eln^{+/-}$ (d) mice. d or diast = diastole; s or syst = systole. $n = 6 – 29$/group. *P < .05 between genotypes.

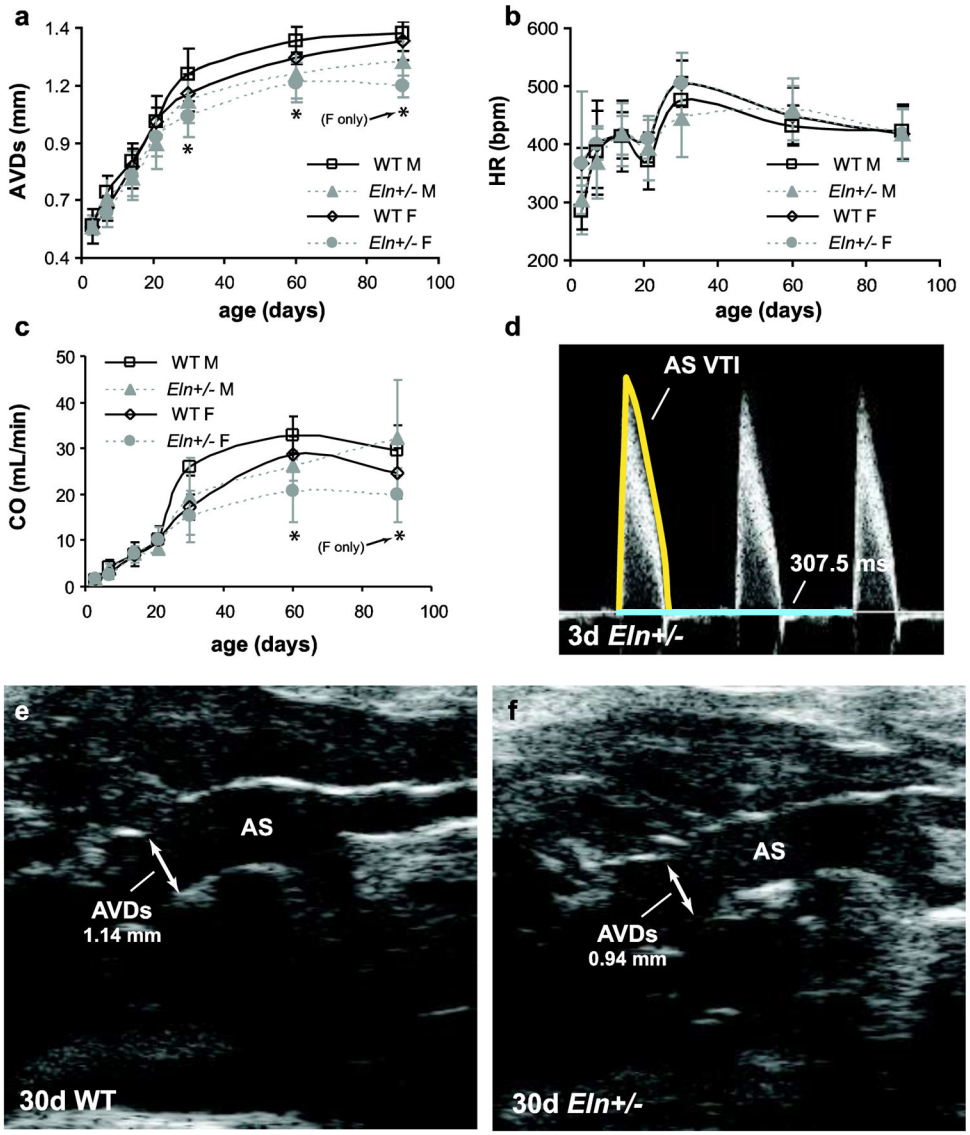

Fig. 5. Dimensions and calculations for cardiac output (CO)

The aortic valve diameter at systole (AVDs) (a) significantly depends on age, sex, and genotype, and is 10% smaller in $Eln^{+/-}$ mice at age 30 and 60d. The heart rate (HR) (b) significantly depends on age and sex, but not genotype. CO (c) significantly depends on age, sex, and genotype, and is 18 – 27% lower in $Eln^{+/-}$ mice at age 60d. Representative Doppler image, velocity time integral (VTI) trace and time measurement of the flow immediately distal to the aortic valve in a 3d $Eln^{+/-}$ mouse (d). Representative b-mode images and diameter measurement of the aortic valve in 30d WT (e) and $Eln^{+/-}$ (f) mice. n = 2–10 males/group, n = 2–15 females/group.

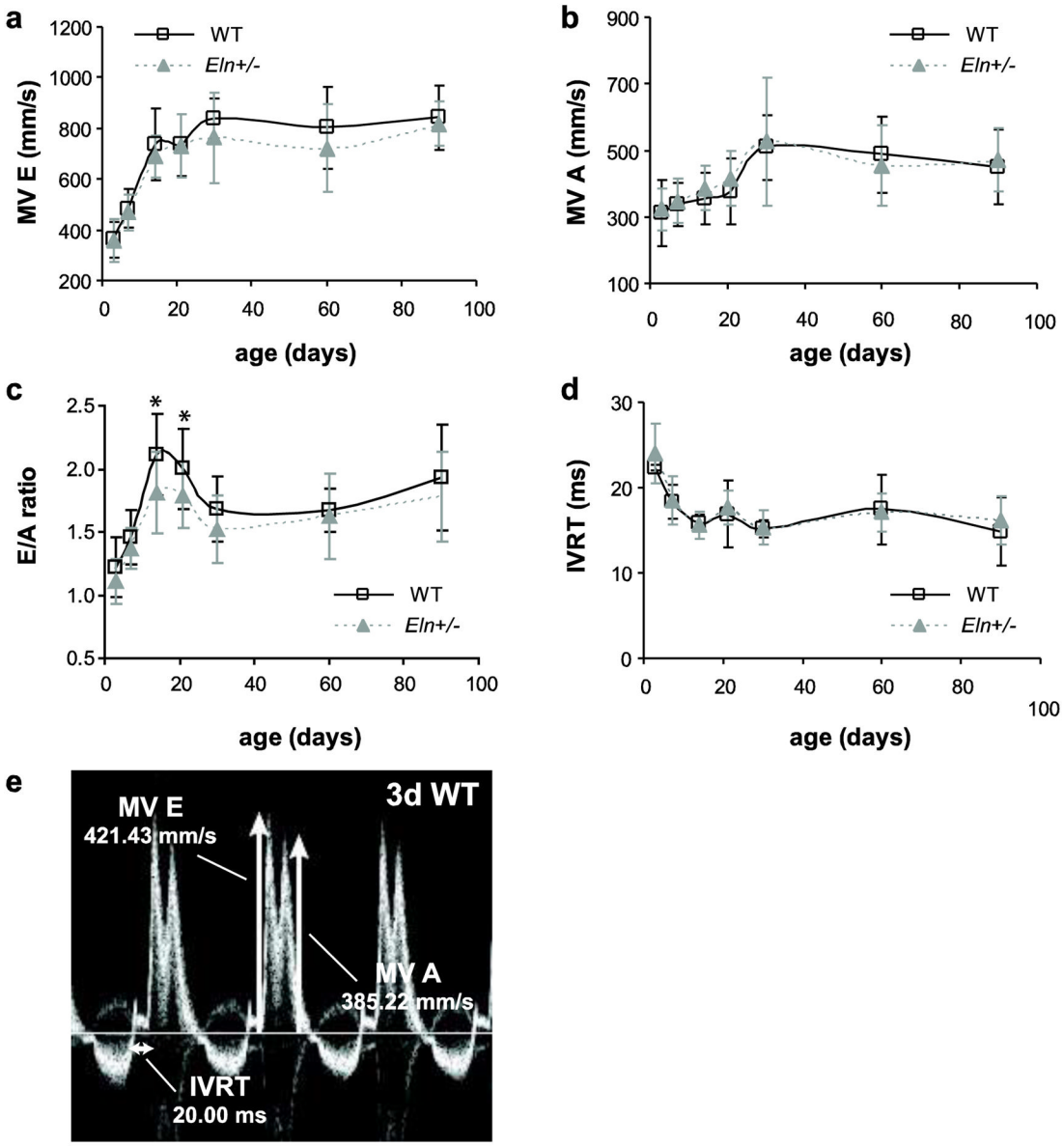

Fig. 6. Dimensions and calculations for ejection fraction (EF)

Left ventricle volume at diastole (LVVd) (a) significantly depends on age and sex, but not genotype. Left ventricular volume at systole (LVVs) (b) significantly depends on age, sex, and genotype. Stroke volume (SV) (c) significantly depends on age and sex, but not genotype. EF (d) significantly depends on age and genotype, but not sex, and is similar between genotypes at all ages except 14d. Representative LV traces at end diastole (e) and end systole (f) for a 3d WT mouse. $n = 6 – 12$ males/group, n = 2 – 17 females/group, $n = 9 – 29$ total/group. *P < .05 between genotypes.

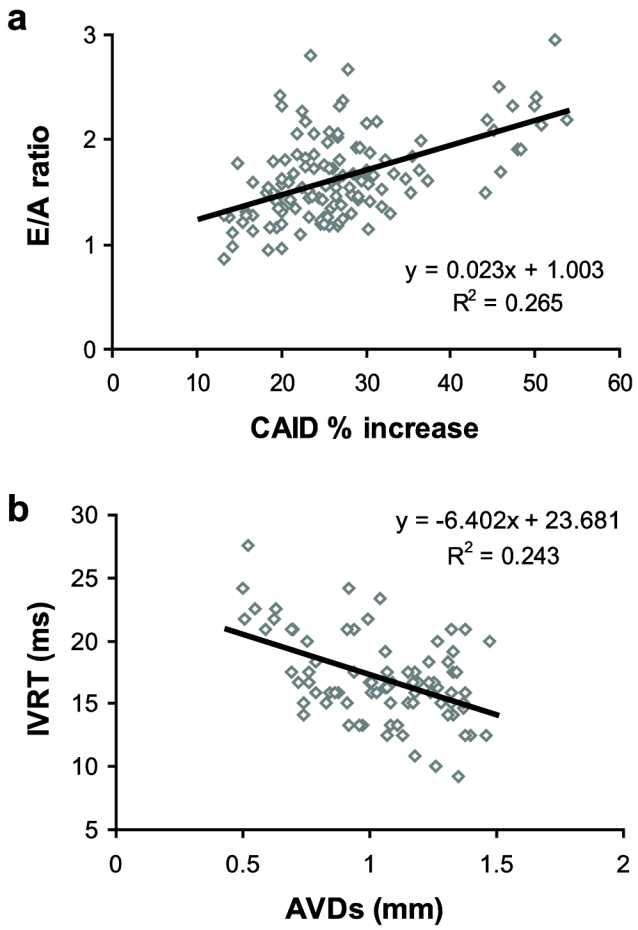

Fig. 7. Mitral valve blood velocities

Mitral valve E wave peak velocity (MV E) (a) and mitral valve A wave peak velocity (MV A) (b) significantly depend on age, but not sex or genotype. E/A ratio (c) significantly depends on age and genotype, but not sex, and is 10–14% lower in *Eln+/−* mice at 14 and 21d. IVRT (d) significantly depends on age, but not sex or genotype. Representative Doppler image with MV E and MV A peak velocity traces, and IVRT measurements for a mitral valve in a 3d WT mouse (e). n = 5–24/group.

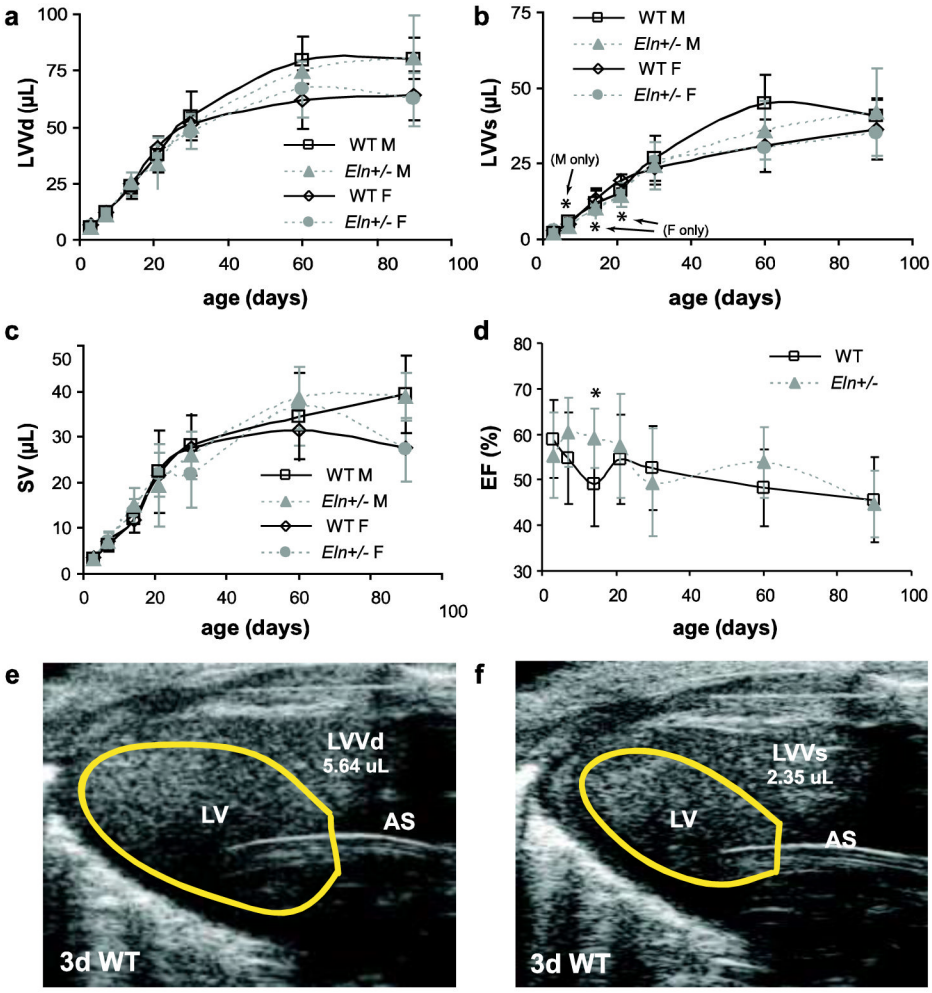

Fig. 8. Correlations between arterial size or compliance and measures of LV diastolic function for all data combined

A measure of arterial compliance (CAID % increase) has a weak, positive correlation with E/A ratio (a). A measure of arterial size (AVDs) has a weak, negative correlation with IVRT (b). Measures of cardiac hypertrophy (LVM/BW) and systolic function (EF and FS) had no correlation with CAID % increase or AVDs.

Table 1

Imaging protocol

Imaging views, abbreviations and calculations used for all results. Adapted from Bose et al. [19].

Parasternal long axis (PSLAX)	
B-mode LV diastolic volume in microliters	LVVd (μL)
B-mode LV systolic volume in microliters	LVVs (μL)
B-mode stroke volume in microliters, calculated	SV (uL)
B-mode ejection fraction, calculated	EF (%)
Parasternal short axis at mid-pap level (PSSAX)	
M-mode LV diastolic inner diameter in millimeters	LVIDd (mm)
M-mode LV systolic inner diameter in millimeters	LVIDs (mm)
M-mode LV diastolic posterior wall thickness in millimeters	LVPWd (mm)
M-mode LV systolic posterior wall thickness in millimeters	LVPWs (mm)
M-mode fractional shortening, calculated	FS (%)
M-mode LV mass in milligrams, calculated - Penn Algorithm [20]	LVM (mg)
Aortic arch view	
B-mode aortic valve systolic diameter in millimeters	AVDs (mm)
M-mode ascending aorta diastolic diameter in millimeters	ASIDd (mm)
M-mode ascending aorta systolic diameter in millimeters	ASIDs (mm)
M-mode ascending aorta diameter percent increase from diastole to systole, calculated	ASID % inc (%)
Modified Parasternal long axis (MPSLAX – alternative)	
B-mode aortic valve systolic diameter in millimeters	AVDs (mm)
M-mode ascending aorta diastolic diameter in millimeters	ASIDd (mm)
M-mode ascending aorta systolic diameter in millimeters	ASIDs (mm)
M-mode ascending aorta diameter percent increase from diastole to systole, calculated	ASID % inc (%)
Suprasternal Notch	
Doppler ascending aorta velocity time integral in centimeters	AS VTI (cm)
Doppler cardiac output in milliliters per minute, calculated [21]	CO (mL/min)
Carotid View	
M-mode common carotid diastolic inner diameter in millimeters	CAIDd (mm)
M-mode common carotid systolic inner diameter in millimeters	CAIDs (mm)
M-mode carotid artery diameter percent increase from systole to diastole, calculated	CAID % inc (%)
Mitral Valve	
Doppler mitral inflow E wave peak velocity in millimeters per second	MV E (mm/s)
Doppler mitral inflow A wave peak velocity in millimeters per second	MV A (mm/s)
E/A ratio, calculated	E/A

Table 2

Results of the general linear model (GLM)

A GLM was used to determine the effects of age, sex, and genotype (GT), and all interactions between these factors on the measured parameters. Significant p-values (< .05) and strong correlations with the linear model ($R^2 > 0.7$) are shown in bold. Because genotype differences with postnatal development are the primary focus of the study, figures always show separate results for each genotype at every age, but only show separate results for male and female mice if sex had a significant effect in the GLM.

Variable	Age	Sex	GT	Age*Sex	GT*Sex	GT*Age	GT*Age*Sex	R^2
BW	**0.000**	**0.000**	0.172	**0.000**	0.650	**0.017**	0.673	**0.969**
LVM	**0.000**	**0.000**	**0.018**	**0.000**	0.972	0.266	0.541	**0.860**
LVM/BW	**0.000**	0.526	**0.037**	0.145	0.623	0.890	0.351	0.263
LVIDdias	**0.000**	0.053	0.433	**0.001**	0.863	0.496	0.707	**0.920**
LVIDsys	**0.000**	0.194	0.448	**0.016**	0.452	0.736	0.859	**0.836**
FS	**0.000**	0.713	0.100	0.557	0.157	0.938	0.925	0.188
ASIDdias	**0.000**	0.244	**0.000**	**0.002**	0.805	**0.039**	0.595	**0.940**
ASIDsys	**0.000**	0.052	**0.000**	**0.002**	0.838	**0.000**	0.757	**0.940**
ASID%inc	**0.000**	0.068	**0.000**	0.065	0.958	0.080	0.681	0.372
CAIDdias	**0.000**	0.878	**0.000**	0.101	0.099	**0.008**	0.414	**0.917**
CAIDsys	**0.000**	0.467	**0.000**	0.370	0.055	**0.001**	0.760	**0.933**
CAID%inc	**0.000**	0.082	**0.000**	**0.029**	0.912	**0.000**	0.411	0.697
AVDs	**0.000**	**0.003**	**0.000**	0.142	0.751	**0.008**	0.904	**0.926**
HR	**0.000**	**0.006**	0.549	0.061	0.307	0.381	0.894	0.388
CO	**0.000**	**0.000**	**0.000**	**0.000**	0.734	**0.000**	0.734	**0.876**
LVVdias	**0.000**	**0.000**	0.199	**0.000**	0.768	0.861	0.800	**0.908**
LVVsys	**0.000**	**0.014**	**0.036**	**0.001**	0.565	0.605	0.444	**0.847**
SV	**0.000**	**0.007**	0.795	**0.000**	0.937	0.099	0.944	**0.812**
EF	**0.000**	0.553	**0.028**	0.382	0.569	**0.041**	0.319	0.282
MV E	**0.000**	0.608	0.121	0.639	0.837	0.829	0.832	0.677
MV A	**0.000**	0.281	0.142	0.108	0.841	0.931	0.873	0.384
E/A ratio	**0.000**	0.651	**0.000**	0.054	0.557	0.565	0.429	0.564
IVRT	**0.000**	0.411	0.488	0.305	0.476	0.953	0.318	0.533